

AUTHOR(S):

TITLE:

YEAR:

Publisher citation:

OpenAIR citation:

Publisher copyright statement:

This is the _____ version of an article originally published by _____
in _____
(ISSN _____; eISSN _____).

OpenAIR takedown statement:

Section 6 of the "Repository policy for OpenAIR @ RGU" (available from <http://www.rgu.ac.uk/staff-and-current-students/library/library-policies/repository-policies>) provides guidance on the criteria under which RGU will consider withdrawing material from OpenAIR. If you believe that this item is subject to any of these criteria, or for any other reason should not be held on OpenAIR, then please contact openair-help@rgu.ac.uk with the details of the item and the nature of your complaint.

This publication is distributed under a CC _____ license.

5th BSME International Conference on Thermal Engineering

Numerical simulation of 2D turbulent natural convection of humid air in a cavity filled with solid objects

Draco Iyi, Reaz Hasan* and Roger Penlington

Northumbria University, Newcastle Upon Tyne, NE1 8ST, UK

Abstract

Natural convection flow in enclosures containing solid objects is important in the design of a wide range of industrial and engineering applications. Numerical calculations were performed for low turbulence double-diffusion convection for humid air inside a rectangular cavity with an aspect ratio of 2:1 (height/width) and partially filled with disconnected solid cylindrical objects occupying 15% of the total cavity volume. The vertical walls are maintained at 1.2 and 21°C and a Rayleigh number of the fluid mixture based on the height of the vertical wall is 1.45×10^9 . In the computations, turbulent fluxes of momentum, heat and mass were modelled by a low-Re (Launder-Sharma) $k-\epsilon$ eddy diffusivity model. Radiation equation was discretised using the discrete ordinate method. Detailed analysis was performed on the flow and heat transfer and on the turbulence quantities within the cavity. The effect of 2D simplification of inherently 3D radiation modelling was carefully scrutinised and calculations carried out with an equivalent emissivity. Variations of average Nusselt number and buoyancy flux are analysed. Profiles of turbulent kinetic energy and turbulent viscosity are studied in detail to observe the net effect on the intensity of turbulence caused by the interactions of radiation with double-diffusive natural convection heat and mass transfer. Particular emphasis was placed on quantifying the proximity of the solid objects to the active walls. It has been found that turbulence is suppressed as the objects get closer to the walls.

© 2013 The Authors. Published by Elsevier Ltd. Open access under [CC BY-NC-ND license](https://creativecommons.org/licenses/by-nc-nd/4.0/).
Selection and peer review under responsibility of the Bangladesh Society of Mechanical Engineers

Keywords: Double diffusive heat and mass transfer; natural convection; emissivity;

1. Introduction

Simultaneous heat and mass transfer in enclosures containing solid objects is important for many practical flows such as indoor environments (Chen and Liu 2004; Ji et al., 2007), drying/cooling of agricultural products (Kadem et al., 2011) and other engineering applications (Laguerre et al., 2005). The basic set up for such flows, which has also attracted attention from both experimental and numerical scientists, is a rectangular cavity whose vertical walls are heated differentially (Tian and Karayiannis, 2000; Didier et al., 2011). Typically, the natural convection heat transfer from the hot to the cold wall is characterised by the formation of a slow moving vortex. This vortical motion is often interpreted as an ‘engine’ which transfers heat from the heated surface (source) to the cold surface (sink) (Bejan, 1993). The intensity of flow is conveniently expressed by the Rayleigh number, $Ra = g\beta\Delta TH^3/\alpha\nu$, where, H is the height of the cavity, β is coefficient of thermal expansion, ΔT is the temperature difference between the vertical walls and α and ν are the thermal and molecular diffusivities of the fluid respectively. Depending on the Rayleigh number the flow can be categorised as turbulent or laminar.

In the last decade or so the trend in buoyancy driven flow research has shifted to the examination of cavity flow coupled with heat and mass transfer. Most of the studies in this category are concentrated on steady state laminar flow of Rayleigh

* Corresponding author.

Email address: reaz.hasan@northumbria.ac.uk

number ranging from 10^4 to 10^6 . Hammou et al., 2004 and McBrain, 1997 investigated temperature and mass concentration gradient induced laminar flow in an enclosure. They used single phase modelling approach for the transport of fluid mixture. It is fairly recently that a number of works have appeared on buoyancy driven flows in enclosures filled with varying numbers of solid objects. Unlike porous medium, these objects are not in contact with each other but are close enough to influence the transfer processes significantly (Das and Reddy, 2006; Laguerre et al., 2009). Most of such works are limited to steady state two dimensional laminar flow of Rayleigh number ranging from 10^5 to 10^9 , although the higher values of Rayleigh number are likely to be turbulent. The flow development is further complicated by the evidence that radiation also plays an important role (Behnia et al., 1990; Iyi et al., 2012) in establishing the flow.

An important aspect of the above type of flow which has not been investigated in detail is the effect on heat and mass transfer due to the wall proximity of blockages. This issue has many practical engineering applications such as natural drying of wood stacks (Kadem et al., 2011), cold storage stacking (Laguerre et al., 2005) or location of venetian blinds in double skin facade (Ji et al., 2007). The objectives of this paper are hence to look at typical features of the heat and mass transfer for variable proximity of the solid objects. The issue of emissivity for radiation simulation has also been explored.

2. Flow domain

The geometrical configuration used in this investigation is similar to the cavity used in the experimental study conducted by Laguerre et al., 2009. As shown in Figure 1, this is a two-dimensional rectangular cavity with aspect ratio of 2:1 (H/L) and contains objects which occupy about 15% of the total cavity volume. The authors have provided data for temperature profiles along the mid-height ($y/H=0.5$) and along $x=6.6$ cm (or $\delta = 6.6$) near the cold wall of the cavity. Vertical velocity and relative humidity profiles measured at the mid-height and mid-width ($x/L=0.5$) of the cavity were also reported.

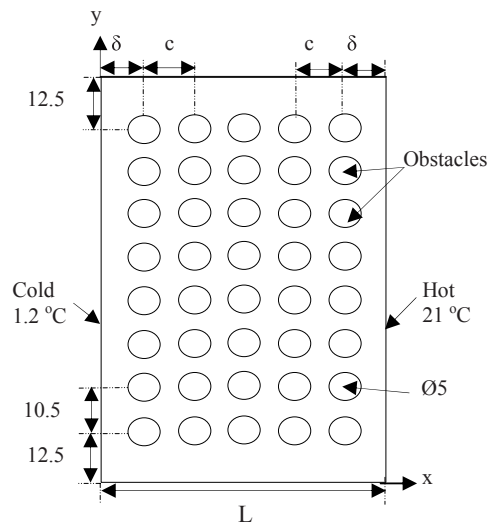


Fig. 1. Geometry and the coordinates (dimensions are in cm)

Based on the temperature differentials of the vertical walls the Rayleigh number was found to be 1.45×10^9 . For this work, the distance of the first column of objects from both the hot and cold walls were varied ($\delta = 0.033, 0.05, 0.066, 0.08$ and 0.116 m). The distances between the other columns, 'c', varies negligibly and hence the effect due to internal re-distribution is ignored.

3. Numerical method

Calculations were carried out using the commercial CFD package of ANSYS FLUENT (2010) software. The methodology involves the iterative solution of the Navier-Stokes equations along with continuity and energy equation on collocated variables within a structured-unstructured mesh configuration. Humidity has been considered as a separate phase and hence another scalar transport equation for species transport has been incorporated. To model the turbulence stresses, a two-equation low-Re eddy-viscosity turbulence model (Launder-Sharma, 1974) has been chosen. Systematic grid dependency tests were carried out and the final results were obtained with 90,500 cells with a y^+ value of just below 1. For a coarser mesh density of 64,600 the average Nusselt number showed very small variation as can be seen in Table 1. Initial natural convection flow field was established for a

Rayleigh number of 10^6 using an incompressible unsteady solver with a time step of 0.002s. This flow field was later used an initial condition for the higher Rayleigh number of 1.45×10^9 . A typical run on a single Intel core 2Duo E6600 2.4 GHz processor took about 8 hours of computing time.

The boundary conditions considered for the simulations are similar to those given in the experimental paper of Laguerre et al., (2009). The temperatures of the hot, cold, top and bottom walls were fixed at 21, 1.2, 14.4 and 13.7°C respectively. The constant vapour mass fraction is maintained at the bottom horizontal wall and a constant mass fraction equal to the saturation value at the cold wall was specified. No slip boundary conditions have been imposed for all the solid surfaces. To simulate radiation, Discrete Ordinate Method (FLUENT 2010) has been chosen with humid air treated as absorbing-emitting and non-scattering gray medium and the walls are all assumed as gray diffuse.

4. Results and discussion

The velocity and turbulence intensity contours shown in Figure 2 (a) and (b) respectively, demonstrate clearly that the main air flow is confined within the boundary layer so that the objects close to the walls interact with the viscous layer. This observation further highlights the importance of using a low- Re model. It can also be seen that there are other streams of flows of varying (smaller) magnitude. Such a flow pattern was also verified and reported in the experimental work of Laguerre et al., 2005 and can be seen in Figure 2.

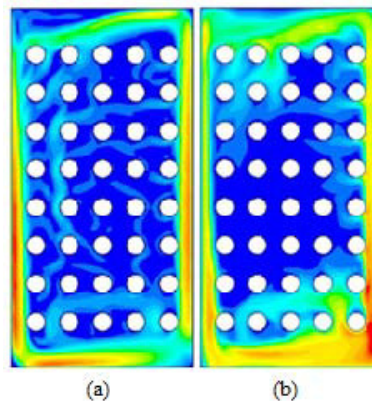


Fig. 2. (a) Velocity magnitude and (b) Turbulence intensity for $\delta = 6.6$ cm

Double-diffusive phenomenon is governed by the total density stratification consisting of thermal and concentration contributions. These two stratifications often act in opposite directions with unstable thermal stratification promoting turbulence, while the stable concentration gradient tends to dampen turbulent fluctuations. In this study, thermal stratification is dominant and is likely to promote turbulence. Specification of the flow regime for such transitional Rayleigh number of 1.45×10^9 associated with heat and mass transfer appears to be quite confusing. To resolve this uncertainty surrounding the flow regime characterisation, preliminary numerical investigation was conducted with Launder-Sharma model to show if the domain is predominantly laminar or turbulent. The temperature profile near the cold wall ($x = 6.6$ cm) is presented in Fig. 3a, and the relative humidity (RH) distribution along the mid-width ($x/L = 0.5$) is presented in Fig. 3b. Both results, laminar and turbulent are plotted against the experimental data which supports our assumption of incorporating a turbulence model in the calculations.

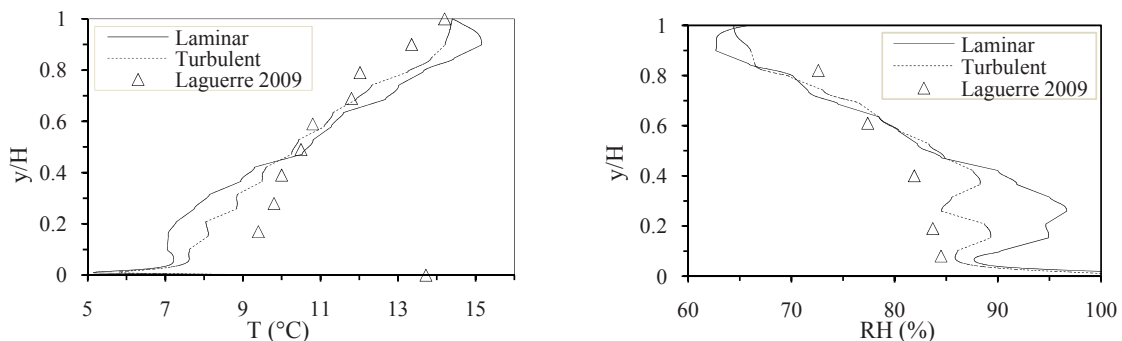


Fig. 3. Comparison with experimental data: laminar vs turbulent prediction ($\delta = 6.6$ cm)

4.1 Choice of equivalent emissivity

The choice of emissivity is very critical when modelling radiation heat transfer and, even for this type of moderate temperature difference, the effect of radiation has been found to be fairly significant (Iyi et al., 2012). The 2D simplification of an inherently 3D radiation heat transfer also raises issues with the accuracy of the data produced by 2D simplification of domain. According to Laguerre et al., 2009 an equivalent emissivity of $\epsilon = 0.58$ can be shown to mimic the radiation heat transfer between three surfaces having emissivities of 0.9 (somewhat similar to the treatment of radiation shield). However, no numerical evidence is provided in support of the above. We have scrutinized this assumption and a comparison of temperature for a 2D vs. 3D domain is presented in Fig. 4. It can be seen that the predicted temperatures at $x/L=0.5$ for $\epsilon = 0.9$ (3D) and $\epsilon = 0.58$ (2D) are in fairly close agreement justifying the 2D treatment. The $\epsilon = 0.9$ (2D) is shown for comparison which also highlights the significant influence of radiation for this flow. All of the calculations reported in this paper were obtained with $\epsilon = 0.58$.

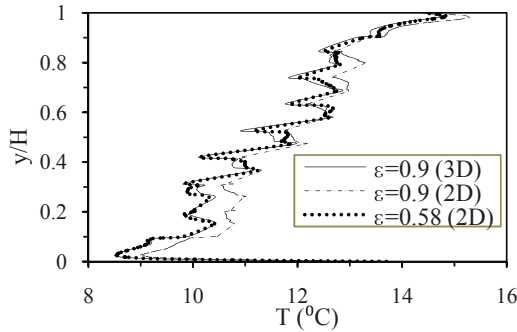


Fig. 4. Emissivity sensitivity for temperature prediction ($\delta = 6.6$ cm)

4.2 Wall heat transfer

Average and local heat transfer data are compared in terms of an average Nusselt number and local Nusselt (Nu_{local}) number computed at each wall. The average Nusselt number which is a combination of heat transfer due to convection and radiation were separately calculated by taking integral averages of heat fluxes using FLUENT post-processing tools. Similarly the local Nusselt numbers were obtained using the local heat flux at each node. Table 1 shows the average Nusselt number for different δ values and Fig. 5 shows local variations for three cases (for clarity).

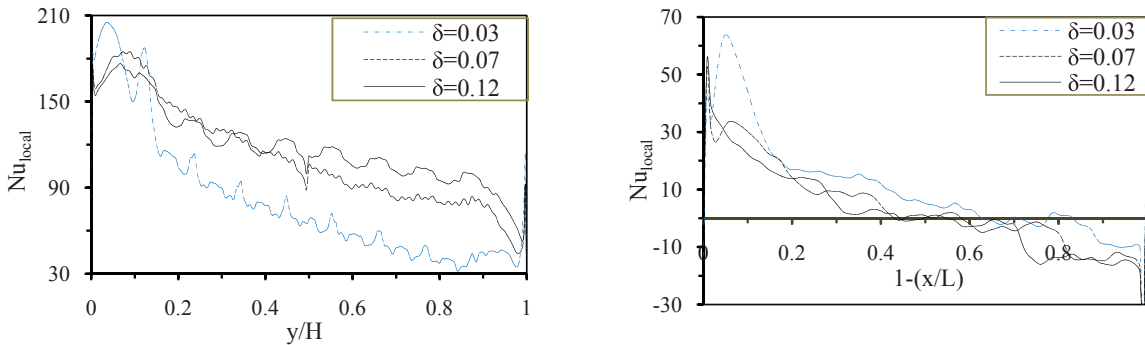


Fig. 5. Variation of local Nusselt number along the (a) Hot wall and (b) Top wall

Table 1: Variation of Average Nusselt Number
(Italicised data for $\delta = 0.066$ are for coarse mesh of 64,600 cells)

δ (m)	Bottom wall	Hot wall	Top wall	Cold wall
0.033	33.8	82	10.4	105.5
0.05	34.1	105.3	7.3	132.1
0.066	30.5(30.4)	111.6(111.3)	3.9(3.8)	138.2(137.8)
0.08	30.4	113.9	2.7	141.5
0.12	29.1	118.5	1.7	146

The table also shows that the total heat transfer is significantly low for the smallest δ value. For other values, the average Nu demonstrates a small but monotonic increase of the heat transfer. The local variations of Nu along the hot wall display the proximity effect very clearly. It also shows that with larger δ values, the Nu numbers tend to smooth out. The fact that $\delta=3.3$ cm shows markedly small value of heat transfer may be partly related to the fact that turbulence is greatly suppressed due to blockage of the upward and downward flow of fluids along the hot and cold walls respectively. The turbulent viscosity ratio, μ_{ratio} (ratio of turbulent eddy viscosity divided by the molecular viscosity) in Fig. 6a-b, highlights that turbulence is greatly reduced as the objects come closer to the walls and supports the multi-zone configuration of flow as suggested by among others, Griffiths and Chen, 2003. For smaller δ , μ_{ratio} is almost close to the core value and hence not shown.

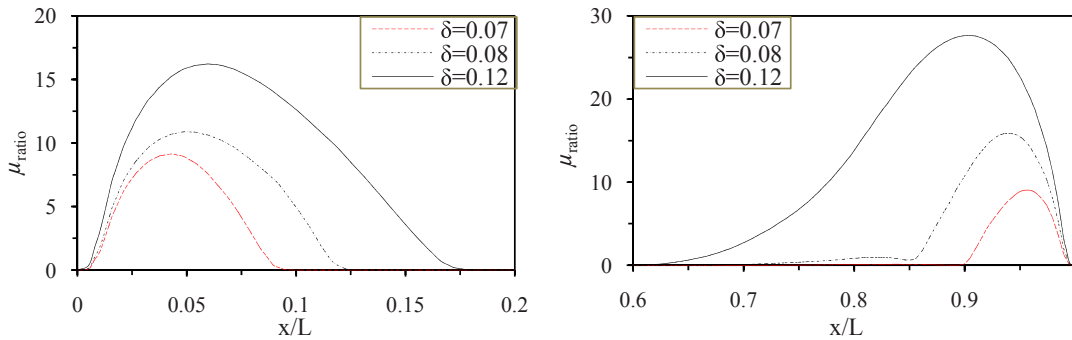


Fig. 6. Turbulent viscosity ratio at the mid-height; (a) near cold wall, (b) near hot wall

4.3 Influence of proximity on mass transfer

Detailed analyses were carried out on the vapour mass flow distributions at various locations of the flow domain. Typical plots of mass fraction, m (g/kg) and buoyancy number, N , defined as the ratio of mass to temperature induced buoyancy, are plotted in Figs. 7 and 8. It can be seen that the mass fraction of vapour increases for the smaller δ values. This is due to the smaller gap available for the flow and is essentially a redistribution of the moisture content throughout the flow domain. The buoyancy number, N , measures the contribution to buoyancy of the variation in vapour concentration. The concentration gradient is due to difference in the relative molecular mass between the dry air and water vapour. At 20 °C, the relative molecular mass of dry air is 28.97 kg/kg-mol, whilst for saturated air it is 28.71 kg/kg-mol. As expected the effect due to mass induced buoyancy is small and corresponds to the trend in Fig. 7.

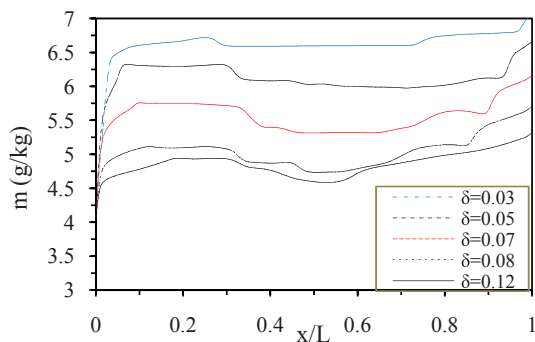


Fig. 7. Mass fraction along the mid-height

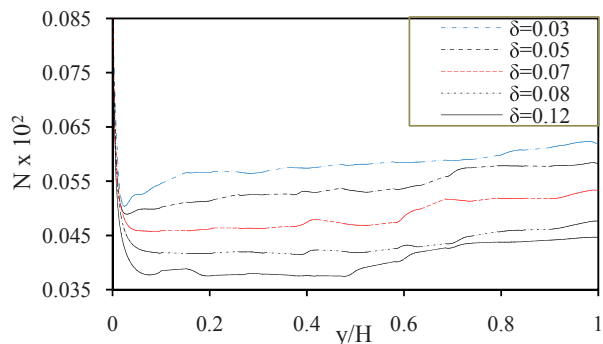


Fig. 8. Buoyancy number along the mid-height

The effective diffusion coefficient, D_{eff} of vapour is shown in Fig. 9a-b at the mid-height. The variations and nature of these curves are very similar to the viscosity ratio curves presented in Figure 6a-b, highlighting the fundamental similarity in the diffusive transport mechanisms of momentum and concentration.

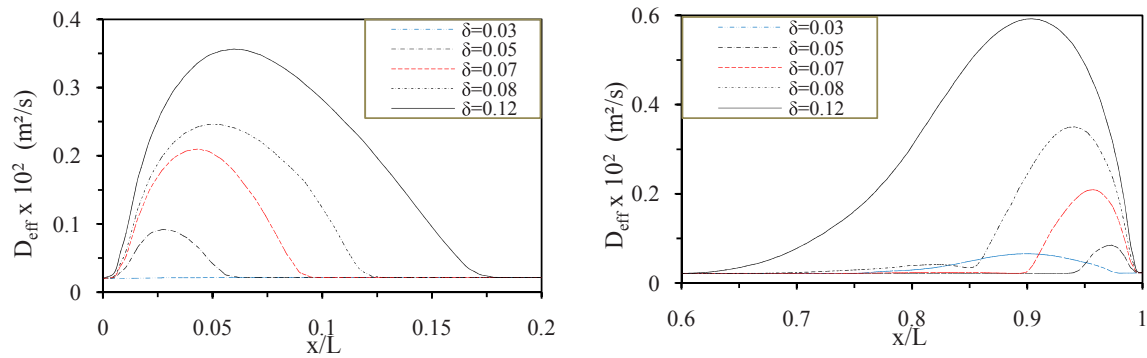


Fig. 9. Effective diffusion coefficient of vapour at mid-height; (a) near cold wall, (b) near hot wall

5. Conclusions

The following conclusions can be made from the work presented above:

- The flow field is characterised by low turbulence near the walls while the core area is essentially a stagnant region.
- Given that an appropriate equivalent emissivity is obtained, a 2D simplification of a 3D domain is possible to save computational effort.
- Wall proximity can be seen to affect the overall heat transfer via flow field. The effect of turbulence is greatly reduced as the gap between the walls and the solid objects become smaller.

References

- [1] Chen W, Liu W. Numerical and experimental analysis of convection heat transfer in passive solar heating room with greenhouse and heat storage. *Solar Energy*, 2004;76: 623–33.
- [2] Ji Y, Cook MJ, Hanby VI, Infield DG, Loveday DL and Mei I. CFD modelling of double-skin facades with venetian blinds. *Proc. Building Simulation*, 2007.
- [3] Kadem S, Lachemet A, Younsi R, Kocaefe D. 3d-Transient modeling of heat and mass transfer during heat treatment of wood. *Int. Communications in Heat and Mass Transfer*, 2011;38:717-22.
- [4] Laguerre O, Ben Amara S, Flick D. Experimental study of heat transfer by natural convection in a closed cavity: Application in a domestic refrigerator. *Journal of Food Engineering*. 2005;70:523–37.
- [5] Tian SY, Karayiannis TG. Low turbulence natural convection in an air filled square cavity. Part II: The turbulence quantities. *International Journal of Heat and Mass Transfer*. 2000;43:867-84.
- [6] Didier S, Rouger N, Francis D, Francois P. Natural convection in an air-filled cavity: Experimental results at large Rayleigh numbers. *Int. Communications in Heat and Mass Transfer*, 2011;38:679-87.
- [7] Bejan A. *Heat Transfer*. New York:Wiley; 1993.
- [8] Hammou ZA, Benhamou B, Galanis N, Orfi J. Laminar mixed convection of humid air in a vertical channel with evaporation or condensation at the wall. *Int. J. Therm. Sci.* 2004;43:531–9.
- [9] McBrain GD. Natural convection with unsaturated humid air in vertical cavity. *Int. J. Heat Mass Transfer*. 1997;40(13):3005-12.
- [10] Das MK, Reddy SK. Conjugate natural convection heat transfer in an inclined square cavity containing a conducting block. *Int. J. Heat Mass Transfer*. 2006;49:4987–5000.
- [11] Laguerre O, Benamara S, Remy D, Flick D. Experimental and numerical study of cavity filled with solid obstacles. *Int. J. of Heat and Mass Transfer*. 2009;25:5691-700.
- [12] Behnia M, Reizes JA, De Vahl Davis G. Combined radiation and natural convection in a rectangular cavity with a transparent wall and containing a non-participating fluid. *Int. J. for Numerical Methods in Fluids*. 1990; 10(3):305-25.
- [13] Iyi DA, Hasan R, Penlington R. Interaction effects between surface radiation and double-diffusive turbulent natural convection in an enclosed cavity filled with solid obstacles. *Proc. of Advances in Computational Heat Transfer, ICHMT*, Bath, UK, 2012.
- [14] ANSYS FLUENT 13.0 (2010).
- [15] Launder BE, Sharma BI. Application of the energy-dissipation model of turbulence to the calculation of flow near a spinning disc. *Letters in Heat and Mass Transfer*, 1974;1:131–8.
- [16] Griffiths B, Chen Q. A Momentum-zonal model for predicting zone airflow and temperature distributions to enhance building load and energy simulations. *HVAC & R Research*. 2003;9(3):309-25.